

# Graphene Assisted Photodegradation of Pollutant Dyes and its Pragmatic Effect on Lemna Minor and Eichhornia Crassipes

Peetam Mandal, Jhuma Debbarma and Mitali Saha\*

Department of Chemistry, National Institute of Technology – Agartala, Jirania, Tripura – 799046, India

(\*) Corresponding author: mitalichem71@gmail.com  
(Received: 4 September 2021 and Accepted: 12 December 2021)

## Abstract

Graphene assisted photodegradation have been used extensively as a remedial measure against pollutant dyes over last few years. The present work highlighted the comparative photodegradation effects between functionalized graphene oxide (GO) and non-functionalized graphene (Gr) maintained at room temperature ( $\sim 27^\circ\text{C}$ ) against three different pollutant dyes viz. malachite green (MG), methylene blue (MB) and methyl orange (MO) under visible light exposure at neutral medium ( $\text{pH} \sim 7$ ). The degradation of MG and MB were remarkably high upon using the functionalized GO while non-functionalized Gr had comparatively less degradation efficiency against both these dyes. On the other hand, Gr was found to be effective than GO in combatting the azoic MO dye due to poor recombination of carrier charges. The photodegradation of 1:1:1 mixture of MG:MB:MO (dye cocktail) was studied in presence of GO, separated in HPLC to estimate the degradation efficiency of each dye. The mineralized products obtained from the LC-MS/MS suggested the fragmentations in each dye occurred via demethylation route followed by asymmetric cleaving. In real-time, the growth assessment of Lemna Minor and Eichhornia crassipes was monitored in dye cocktail alone and in presence of GO treated dye cocktail.

**Keywords:** Graphene, Graphene oxide, Photodegradation, Malachite green, Methylene blue, Methyl orange, Aquatic plants.

## 1. INTRODUCTION

Graphene assisted photodegradation has been proved a renowned remedial measure against pollutant dyes, nowadays [1-6]. The low bandgap energy, high surface area and electron mobility of various metallic nano-photocatalysts is quite well-established and fruitful for dye removal in recent times [7-11]. Attractively, the incorporation of various functionalized graphene derivatives with metallic photocatalysts has been advantageous in further reducing bandgap energy and suppressing charge recombination for these composite materials [12-14]. The  $\pi$ - $\pi$  conjugated structures of graphene and its derivatives causes rapid visible light-induced exciton separation as well as slow charge recombination in electron-transfer processes enhancing the degradation

efficiency towards pollutant dyes. However, direct usage of non-functionalized graphene in photodegradation is extremely limited due to its high hydrophobicity and inert chemical nature.

Irrespective of diverse classification of dyes based on active chromophore, chemical structures and nature, dyes in any form either vat, acidic, basic or azoic hinder anthropogenic activities or impose chronic, carcinogenic and mutagenic effects on aquatic flora and fauna [15-21]. The removal of these environmental malevolent dyes essentially requires cleaving their complex structures using an eco-friendly material under normal atmospheric condition. The high colour intensity, solvation energy and resonance

stabilized structure of malachite green (MG) and methylene blue (MB) makes them highly soluble, non-biodegradable, teratogenic and neurotoxic for living organisms [22-24], whereas the complex azoic (-N=N-) structure of MO is solely responsible for apoptosis on nephron, liver cells and dermatitis in pubescent children [25, 26].

In order to assess the degradation efficiency of hydrophilic and hydrophobic structures within the graphenic lattice, both functionalized and non-functionalized graphene were chemically synthesized from dextrose at ~ 135–145° C under normal atmospheric condition [27]. The present work highlighted the utilization of these chemically synthesized functionalized graphene oxide (GO) and non-functionalized graphene (Gr) to study the photodegradation capability towards MG, MB and MO under visible light at neutral pH. Further, the real-time effect of GO treated dye water on *in-vitro* growth of Water Hyacinth (*Eichhornia crassipes*) and Common Duckweed (*Lemna Minor*) was also discussed.

## 2. EXPERIMENTAL

### 2.1. Materials and Methods

Dextrose was bought from E. Merck while all the dyes viz. MG, MB and MO were purchased from Alfa Aesar while acetonitrile and ortho-phosphoric acid were obtained from JT Baker. Graphene oxide (GO) and graphene (Gr) were synthesized in a single step by heat treatment of dextrose at 135 – 145° C [27]. The 6-membered carbon ring of dextrose produced GO in presence of trace amount of air whereas it gave Gr in presence of thiourea.

### 2.2. Instrumentation

High Resolution Transmission Electron Microscopy (HRTEM) images of the synthesized GO and Gr were acquired in JEM 2100F microscope with an acceleration voltage of 300 kV. The absorbance spectra was recorded using

Cary 60 | Agilent Technologies UV-Vis spectrophotometer at a scan range of 200-800 nm. Waters Alliance® HPLC with e2695 separation module coupled with 2998 PDA detector was used for the rate kinetics and separation of three dyes designating the undermentioned operational parameters. Mobile phase: A, 0.1% H<sub>3</sub>PO<sub>4</sub> in acetonitrile, B, 0.1% H<sub>3</sub>PO<sub>4</sub> in water, flow rate: 1 ml per min, Column: RPC18 Agilent made, λ: 620 nm for MG, 662 nm for MB, 503 nm for MO. The gradient program was as follows: 0 – 4 min @ 1 ml per min flow rate with A – 40% and B – 60%, then 4 – 4.5 min A – 60% and B – 40%, 4.5 – 8 min A – 60% and B – 40%, then 8 – 9 min A – 60% and B – 60% and finally run from 9 – 15 min with A – 40% and B – 60%. The HPLC separation was coupled with AB Sciex Triple Quad 5500, Agilent Technologies mass spectrometer to study the dye fragments. The spectrometer was equipped with electro-spray ionization (ESI) source and functioned at both positive and negative polarity. The ESI conditions were customized as follows: capillary voltage: 5.5 kV in positive and -4.5 kV in negative, nebulizer pressure at 70 psi while the mass range was from 50 to 600 Da.

### 2.3. Photodegradation Studies Under Visible Light Illumination

The photodegradation capability of both GO and Gr were studied against three pollutant dyes viz., MG, MB and MO under exposure of commercial 40-Watt Wipro visible-light induced LED lamp. 100-ppm aqueous solution of each dyes were prepared, separately followed by the addition of GO and Gr (100 mg each), to the dye solutions. A mixture of MG, MB and MO (1:1:1) was also prepared to estimate the degradation efficiency and study the photodegrading ability of GO. The retention time (r.t.) of freshly prepared standard solutions of MG, MB and MO were found to be 8.628, 3.701 and 4.567 mins, respectively and the mineralized dye products were analyzed in LC-MS/MS.

## 2.4. Pragmatic Application of Dye Mixture and Dye Treated Water with GO

The standard dye mixture and the photodegraded water using GO were utilized to study the *in-vitro* growth of Common Duckweed (*Lemna Minor*) and Water Hyacinth (*Eichhornia crassipes*) at optimum temperature ( $\sim 27^\circ\text{C}$ ). Prior to *in-vitro* growth investigation, both the aquatic plants were obtained from Lake Rudrasagar, Tripura, India ( $23.5004^\circ\text{N}$ ,  $91.3168^\circ\text{E}$ ).

## 3. RESULTS AND DISCUSSION

### 3.1. Photodegradation Process Under Commercial Visible Light Illumination

Dextrose was found to produce GO in presence of trace amount of air while Gr in presence of thiourea at the same temperature. The thiourea prevented the attack of atmospheric oxygen during the formation of graphenic lattice. The HRTEM images of GO and Gr in fig. S1a and b, respectively demonstrated the formation of nanosheets. The comparative photodegradation behaviour of GO and Gr was studied against three pollutant dyes at neutral pH as shown in fig 1-3. It is prevalent that the functionalized graphene derivatives are effective against photodegrading pollutant dyes due to rapid electron mobility, higher electron mobility and larger surface area than pristine graphene [28-30]. GO was found to degrade MG drastically ( $\sim 95.95\%$ ) after 7 h whereas Gr showed degradation efficiency of  $\sim 84\%$  after 7 h (fig. 1a-c). It indicated that the hydroxyl (-OH) and carbonyl (C=O) facilitated rapid electron mobility. However, upon illumination of visible light, both GO and Gr did not yield any degradation in dark condition.

The relative peak area was plotted using HPLC chromatogram with the usage of GO and Gr against degradation of MG, correspondingly where the r.t. of MG was 8.628 mins at 620 nm confirming the rapid photodegradation over irradiation time (fig. 1d, e). Both GO and Gr formed

multiple mineralized products of MG on various wavelengths of the HPLC chromatograms @ r.t.  $\sim 2-4$  mins which proved the degradation ability of both the materials. The pseudo-1st order rate was calculated with linear fitting slope of  $\ln(C_0/C)$  vs  $t$  for GO and Gr and the apparent rate constant ( $k$ ) was found to 0.0116 and  $0.00434\text{ min}^{-1}$ , respectively (fig. 1f). The applicability of this pseudo-1st order kinetics model with GO and Gr was found to strongly correlate with Pearson's coefficient value ( $R$ ) of 0.89017 and 0.90254, respectively [31].

Under visible light illumination, MB degraded in presence of 100 mg of GO and Gr, separately at neutral pH with degradation efficiency of  $\sim 90.1$  and  $83.6\%$  for GO and Gr, respectively (fig. 2a, b). The relative degradation calculations further justified that both GO and Gr performed efficiently under the influence of photons and therefore did not promote degradation of MB under dark condition (fig. 2c). The r.t. of MB @ 662 nm was found to be 3.701 mins upon decolorizing with GO and Gr (fig. 2d, e). The chromatogram of MB degraded with GO, was in good accordance with its corresponding UV-absorbance spectra (inset, fig. 2d). Langmuir-Hinshelwood model was applied to extrapolate the pseudo-1st order rate kinetics ( $k$ ) equation using the rate equation (fig. 2f):  $\ln(C_0/C)$  vs  $t$  where  $C_0$  is the initial concentration of MB and  $C$  is the final concentration of MB,  $k$  is the apparent rate constant and  $t$  is the irradiation time [32]. The  $k$  for MB was found to  $0.00372$  and  $0.0052\text{ min}^{-1}$  respectively in case of GO and Gr. The correlation co-efficient  $R$  were 0.98488 and 0.97646, correspondingly further supported the pseudo-1<sup>st</sup> order rate kinetics of MB.

As evident from the literature, functionalized graphene derivatives are more prominent to degrade most of the pollutant dyes like MG and MB as compared to non-functionalized graphene derivatives [33-36]. But in contrast to the

literature azo dyes tend to produce several adducts which hinder its degradation [37-39]. The same phenomenon was observed in case of GO and Gr also. Surprisingly, non-functionalized Gr was found to be more capable to degrade the azoic MO dye

(74.5 %) while GO was found to degrade only ~ 43.4% at neutral pH under the influence of visible light (fig. 3a-c). It is attributed to the fact that fast recombination rate ( $h^+ + e^-$ ) always leads to poor degradation efficiency [40, 41].

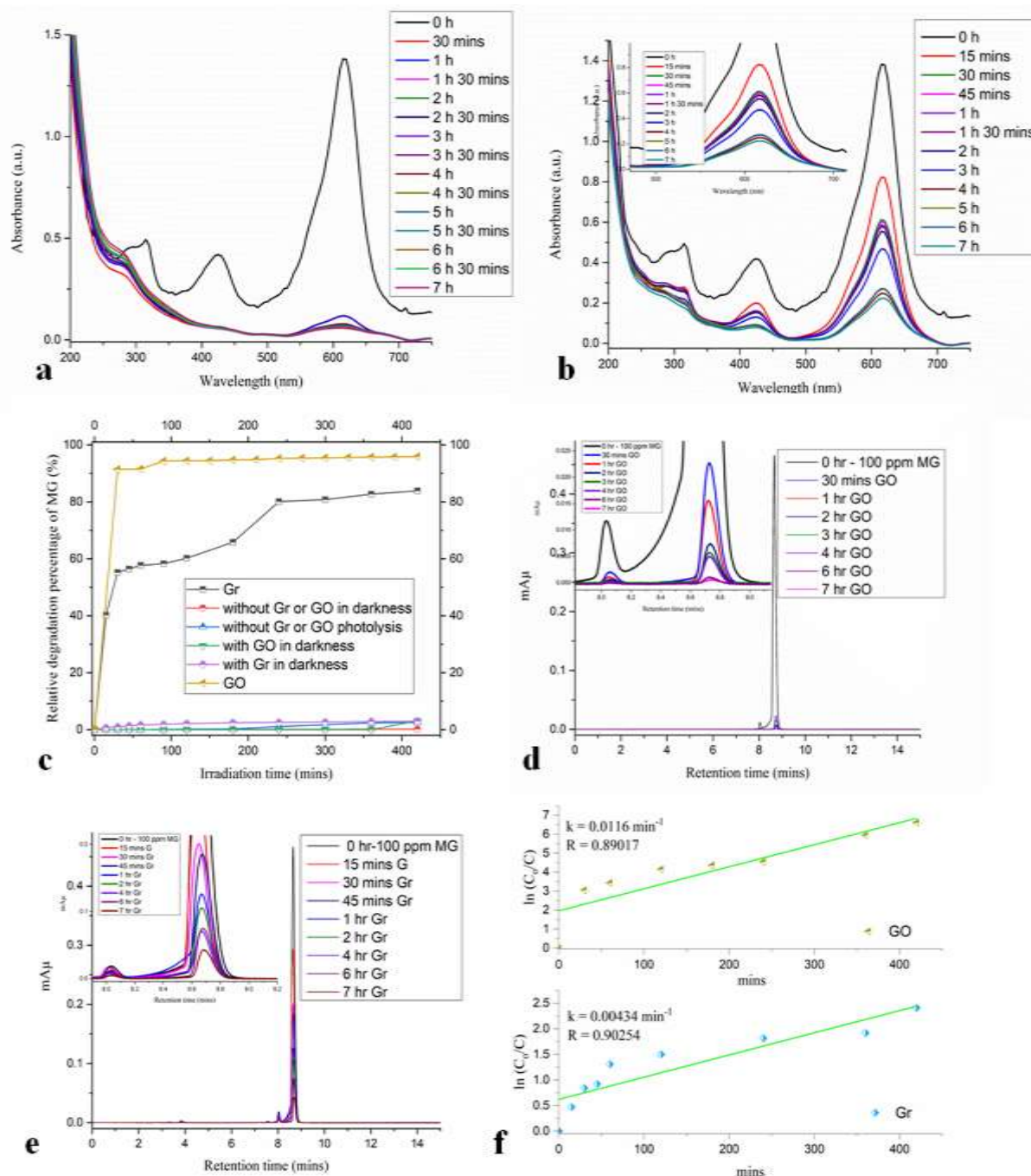


**Figure 1.** Photodegradation of MG under visible light illumination at  $pH \sim 7$ . Absorbance spectra of MG degraded with (a) GO and (b) Gr. (c) Degradation percentage of MG under variable condition. HPLC of MG degradation by (d) GO and (e) Gr. (f) Pseudo 1st order kinetics of MG using GO and Gr.

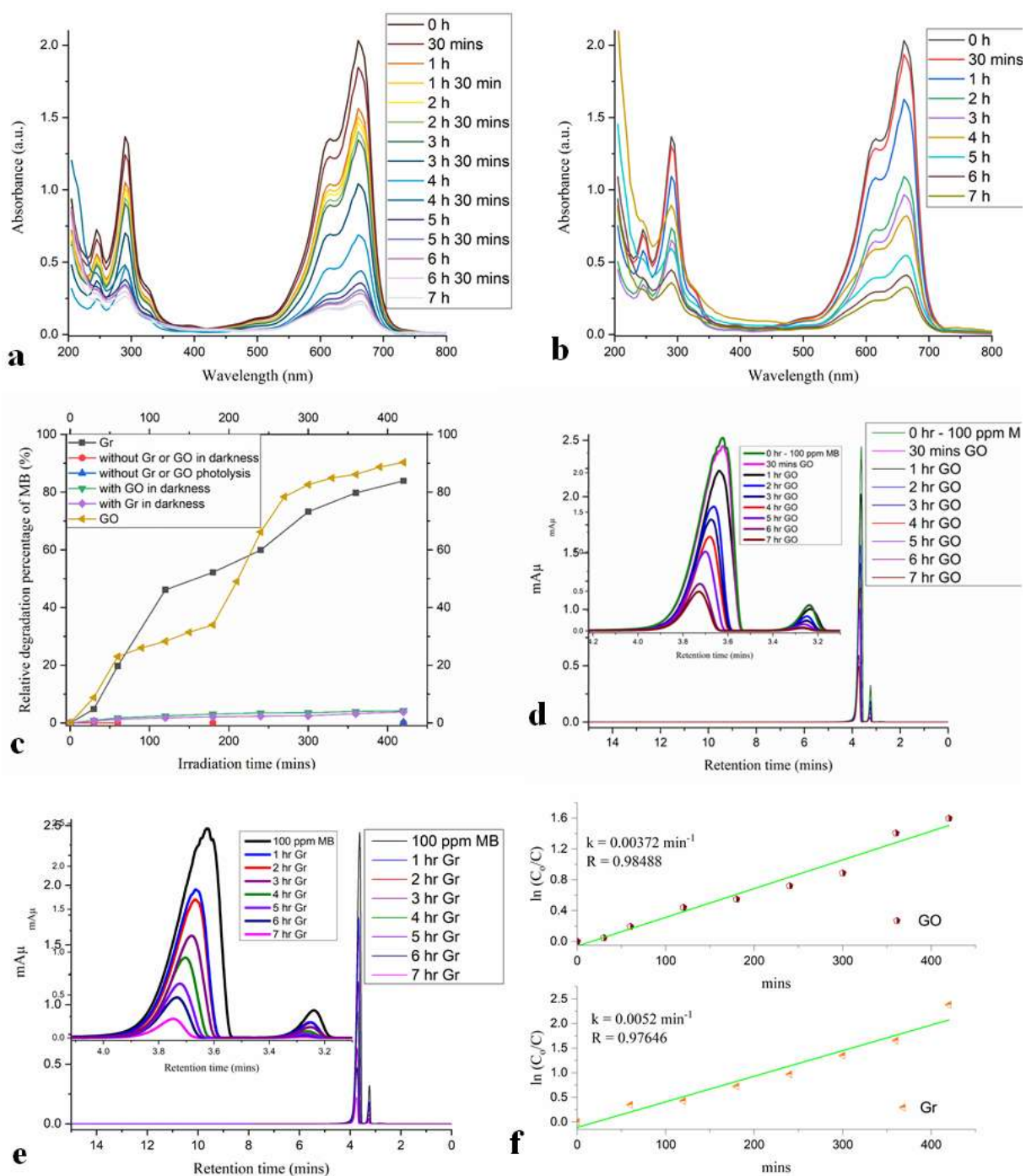


**Figure 2.** Photodegradation of MB under visible light illumination at pH ~ 7. Absorbance spectra of MB degraded with (a) GO and (b) Gr. (c) Degradation percentage of MB under variable condition. HPLC of MB degradation by (d) GO and (e) Gr. (f) Pseudo 1st order kinetics of MB using GO and Gr.

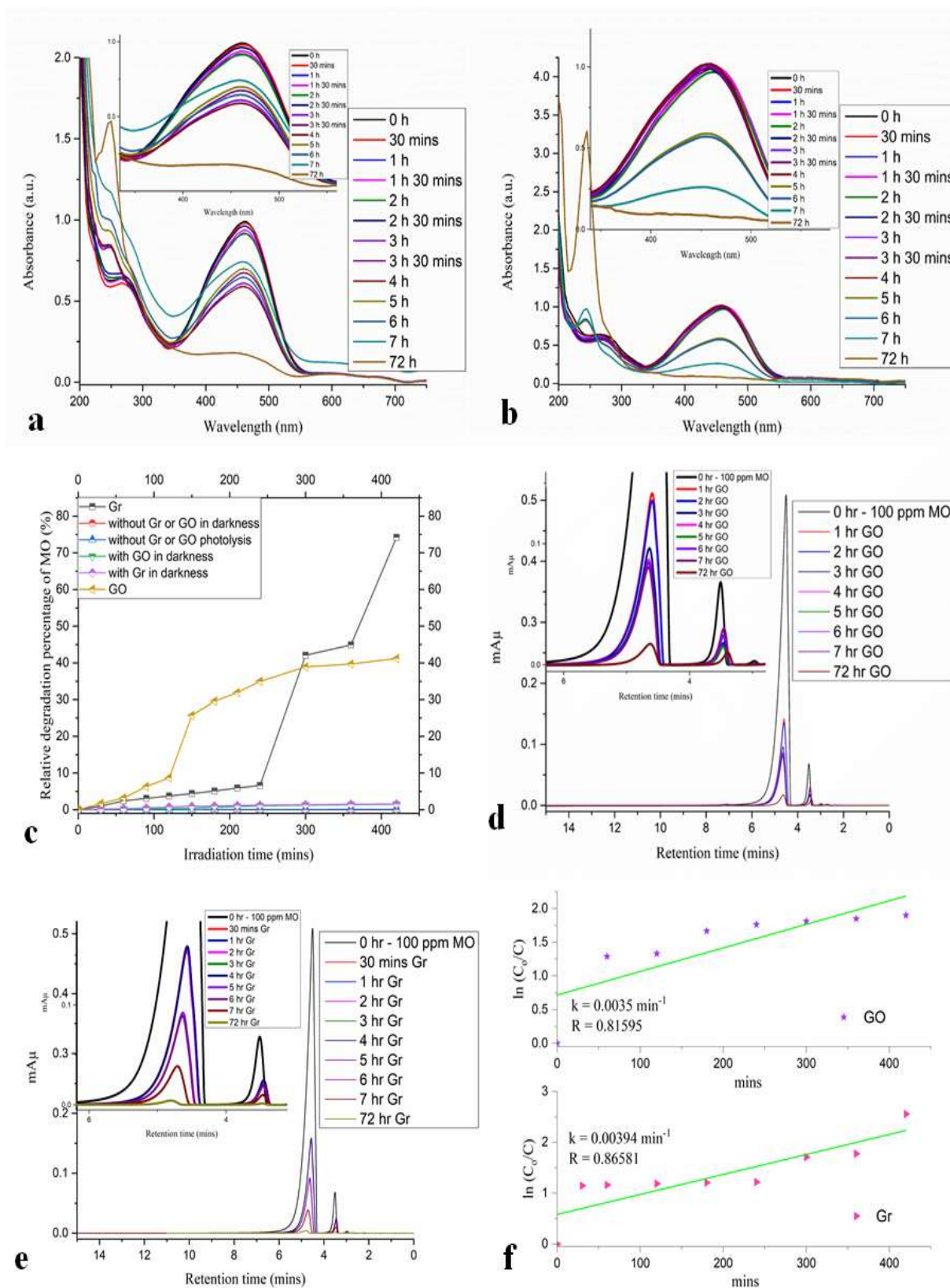


**Figure 3.** Photodegradation of MO under visible light illumination at pH ~ 7. Absorbance spectra of MO degraded with (a) GO and (b) Gr. (c) Degradation percentage of MO under variable condition. HPLC of MO degradation by (d) GO and (e) G. (f) Pseudo 1st order kinetics of MO using GO and Gr.

This might be due to the high recombination effect of functional groups present in GO with the azo-bonds (-N=N-), anions, dual phenyl rings and multiple bonds within MO, leading to poor degradation efficiency. On the other hand, the  $\pi$ - $\pi$  conjugation within the Gr increased the electronic charge which prohibited the recombination. The corresponding HPLC chromatograms @

503 nm with r.t. of 4.567 mins strengthened the UV absorbance spectra of MO degraded with GO and Gr (fig. 3d, e). The pseudo-1st order rate constant  $k$  was 0.0035 and 0.00394  $\text{min}^{-1}$  respectively, for MO degraded with GO and Gr (fig. 3f). The correlation co-efficient  $R$  were 0.81595 and 0.86581 for GO and Gr, correspondingly further supported the pseudo-1st order rate kinetics of MO.

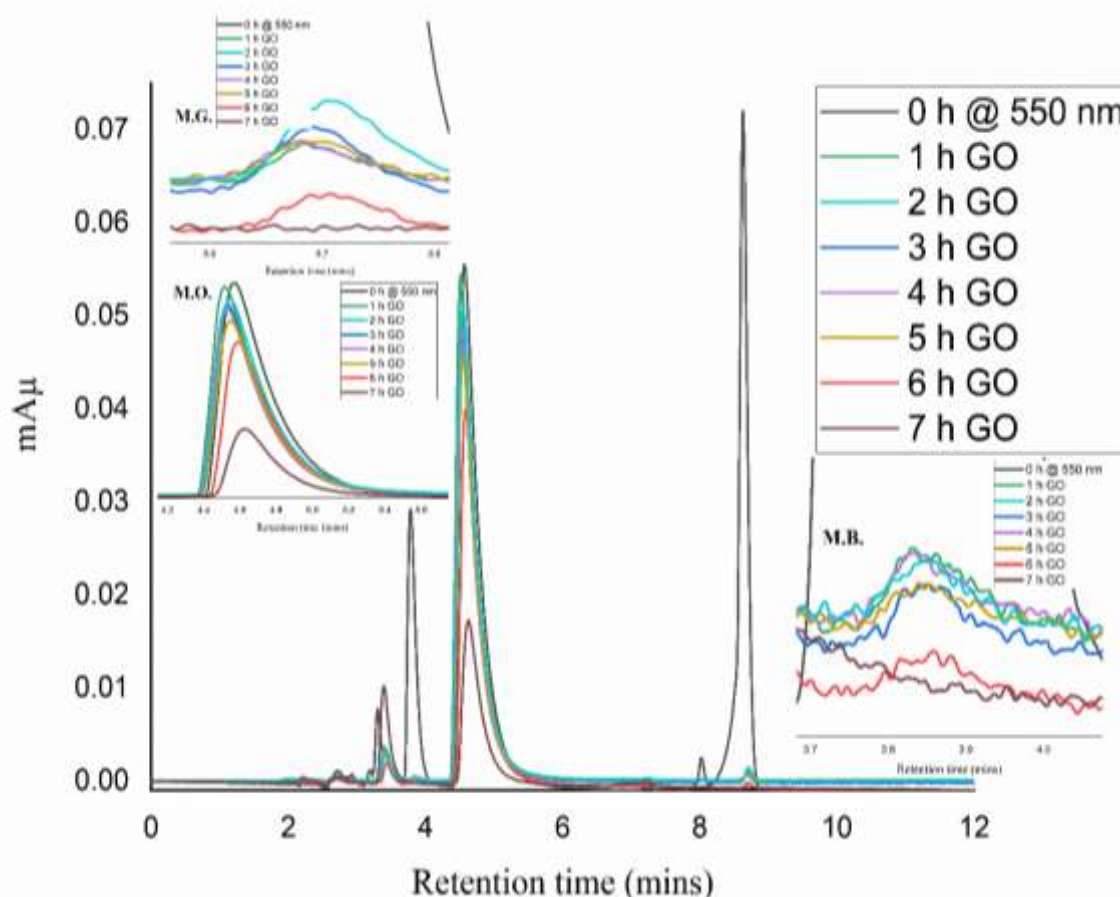


**Figure 4.** HPLC of dye mixtures degraded with GO under visible light illumination at pH ~ 7.

In order to increase the degradation efficiency of GO towards this azoic dye, the photodegradation of 1:1:1 mixture of MG:MB:MO was studied and was separated in HPLC to estimate the degradation efficiency of each dye (fig. 4). The degradation efficiency of GO towards MO increased from 43.4% to ~ 70% after 7 h of stirring under visible light exposure. The photodegradation of MG and MB also

increased up to ~ 97.97% and ~ 98.1% within 1 h in presence of GO.

The comparative tabular representation in table 1 demonstrated the characteristic photodegradation process of MG, MB and MO removal with other reported processes. This concluded that the chemically synthesized GO with a dosage amount of 100 mg was promising in the removal of high concentrated (100 ppm) amount of these three pollutant dyes at pH 7.

**Table 1.** Comparison of present study with previous materials reported for removal of MG, MB and MO dye.

Process	Material	Dye	pH	Amount of material	Time (mins)	Degradation Efficiency (%)	Ref.
Biosorption	Modified fruit pericarp	MO	4	0.6 g/L	1440	<90	[21]
Adsorption	GO	MG	-	42.4 µg/mL	-	25.65	[42]
Photodegradation	Cellulose Acetate-GO	MB	2	10 mg	250	90	[43]
Adsorption	GO	MO	2	1000 mg	150	88	[44]
Adsorption	Pt-Co/GO	MB	10	32 mg/L	90	91	[45]
Photodegradation	AgBr/g-C <sub>3</sub> N <sub>4</sub>	MO	5.5	430 mg	60	-	[37]
Photodegradation	GO	MG	7	100 mg	60	97.97	This study
Photodegradation	GO	MB	7	100 mg	60	~98	This study
Photodegradation	GO	MO	7	100 mg	420	~70	This study

### 3.2. Studies of Dye Fragments After Photodegradation with GO

The mineralized products obtained from various dyes i.e., MG, MB and MO were analyzed by LC-MS/MS and the degradation pathway was proposed based on the mass spectral data (fig. 5, 6). GO fragmented MG into 4-((4-aminophenyl) (phenyl)methyl)-N-methylaniline (Y,  $m/z = 289$ ) via demethylation within 30 mins of stirring under visible light illumination at neutral pH [46]. Whereas 7 h of stirring led to hydrolysis followed by asymmetric cleavage of MG into final product formation, 4-(dimethylamino) phenol (Z,  $m/z = 138$ ) (fig. 5a, b) [46, 47]. In contrast to literature, where MG had been degraded with the formation of several adduct products [48, 49], the chemically synthesized GO had immense potential to mineralize the highly resonance stabilized triphenyl structure of MG into lower molecular weight product.

Contradicting to the photodegradation of MG having major product, GO produced multiple fragments in case of MB after 5 h of stirring under visible light at pH 7. The intermediates were thionin (M,  $m/z = 226$ ); 2-amino-5-

(methylamino) benzene sulfonic acid (N,  $m/z = 208$ ) and (S)-3-aminocyclohexa-2,4-diene-1-sulfonic acid (O,  $m/z = 175$ ) (fig. 5c, inset) [50-52].

The fragment M resulted from demethylation of MB, whereas the hydroxyl (OH<sup>•</sup>) radical generated from GO further fragmented the complex anthracene like structure of MB into N and O via demethylation and asymmetric cleaving. However, the completion of photodegradation of MB after 7 h, resulted into formation of single product i.e., N<sup>1</sup>, N<sup>1</sup>-dimethylbenzene-1,4-diamine (M,  $m/z = 226$ ) (fig. 5d).

In contrast to the mineralization of both the basic dyes MG and MB, 7 h of stirring with GO under visible light exposure produced several multiple adducts of the azoic MO dye having  $m/z > 327$  (fig. 6a). After 7 h of stirring in presence of GO, the major fragments were benzene (A,  $m/z = 78$ ); 4-hydrazineyl-N,N-dimethylaniline (B,  $m/z = 152$ ); 2-(dimethylamino)-5-hydrazineylphenol (C,  $m/z = 167$ ); (S)-4-aminocyclohexa-2,4-diene-1-sulfonic acid (D,  $m/z = 175$ ); sodium 4-hydrazineylbenzenesulfonate (E,  $m/z = 207$ ); 4-(((E)-2-methylbut-2-en-1-

yl)diazenyl)benzenesulfonic acid (F,  $m/z = 253$ ) and sodium 4-((4-aminophenyl)diazenyl) benzenesulfonate (G,  $m/z = 297$ ) (fig. 6b) [53-56]. The formation of the bulky fragment G via demethylation indicated conversion of 3° amine into 1° amine at neutral pH whereas other fragments generated from asymmetric

cleavage of MO. Irrespective of different chemical structures of MG, MB and MO yet the fragmentation occurred with initial demethylation route and further the presence of OH· radical heterolytically cleaved all the dyes into smaller intermediates after 7 h.

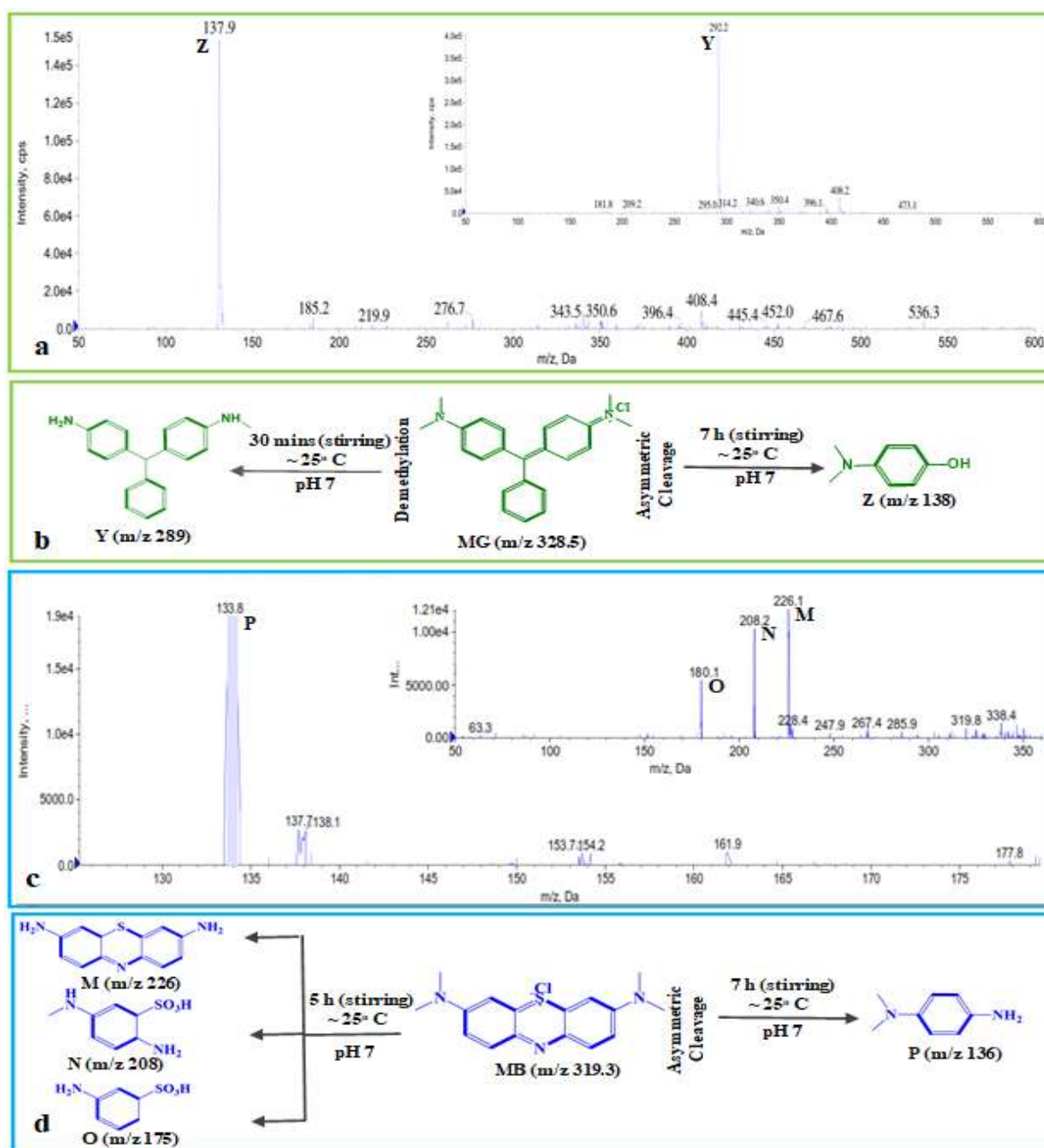


**Figure 5.** Mass spectra of MG after (a) 7 h and 30 min (inset) of stirring with GO and (b) logical degraded fragments of MG at different time intervals. Mass spectra of MB after (c) 7 h and 5 h (inset) of stirring with GO and (d) logical degraded fragments of MB at different time intervals.

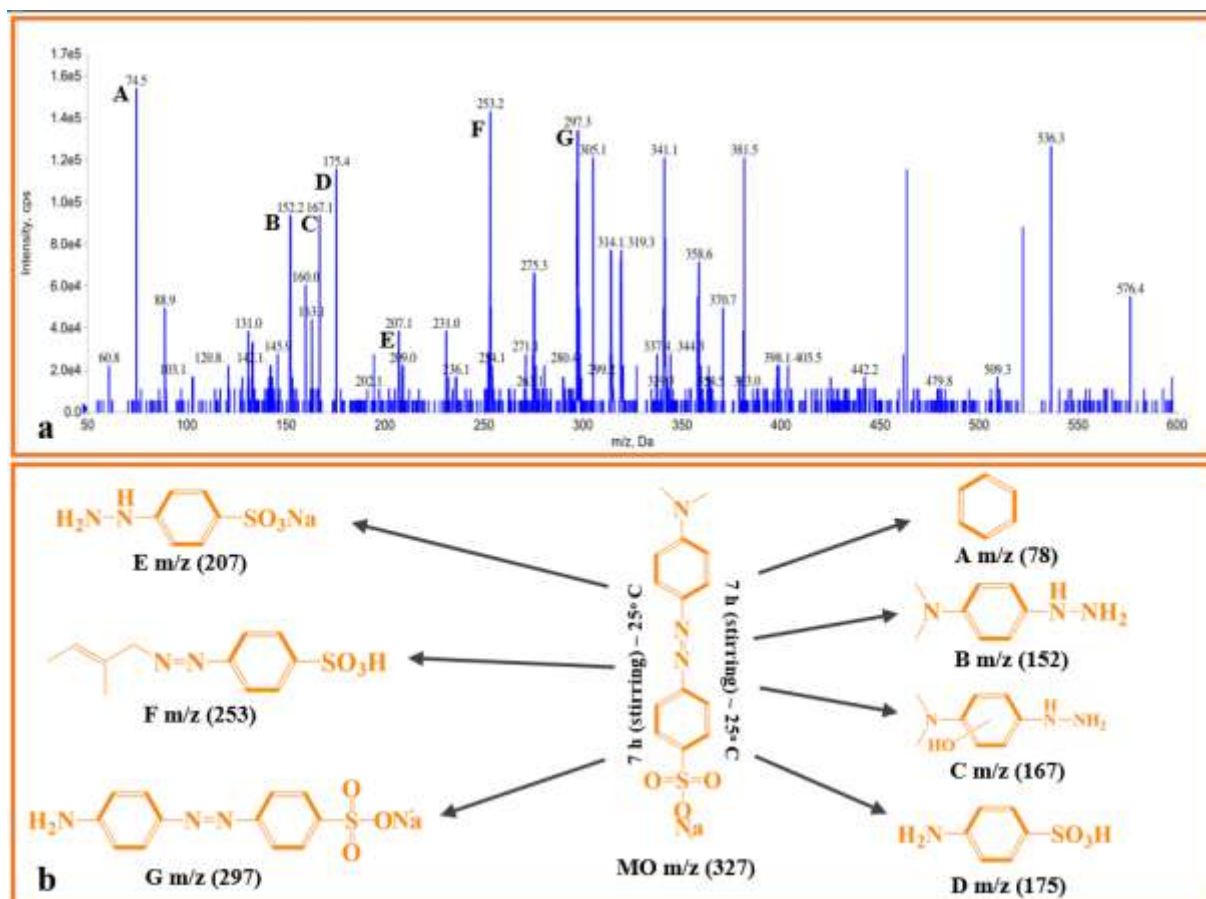


**Figure 6.** Mass spectra of MO after (a) 7 h stirring with GO and (b) logical degraded fragments of MO.

### 3.3. Pragmatic Application on Perennial Aquatic Plants

The presence of Lemna Minor in stagnant freshwater has extensive phytoremediation characteristics against heavy metals [57, 58]. It was observed that 1:1:1 mixture of MG: MB: MO totally stopped the growth of Lemna Minor, as the aquatic weed did not show any significant growth up to 20th day. However, the dye mixture treated with GO showed rapid in-vitro growth proliferation within 15 days (fig. S2a, b). In a similar trend, the growth of Eichhornia crassipes was monitored in dye mixture alone and GO treated dye mixture. Even though it is known to resist highly acidic and alkaline condition [59, 60], yet the plant started to bloat from day-2 in dye mixture clearly indicating visual signs of decomposition. The active decaying started from 3rd day and after a week complete decay occurred (Fig. S3a). Fascinatingly, GO treated dye

mixture proved to be an elixir for the in-vitro sustainable growth of this ornamental Eichhornia crassipes at room temperature  $\sim 27^\circ \text{C}$  with ad libitum access to sunshine (fig. S3b). On the 10th day, the embryonic stem (hypocotyl) thickened and new roots started to shoot while on day-15, the hypocotyl extended with the emergence of new leaf from cotyledon. The aquatic weed was transferred to bigger container after carefully pruning the roots and radicles within 30 days. After that, flowering as well as sprouting of new embryonic roots were observed which confirmed that the dye treated water could be safely applied for sustainable harvesting Eichhornia crassipes even up to 2 months.

### 4. CONCLUSION

It has been observed that both the functionalized GO and non-functionalized Gr has immense potential to degrade pollutant dyes viz. MG, MB and MO under

visible light irradiation at neutral pH. GO degraded MG and MB with a degradation efficiency of ~ 95.95 and 90.1%, respectively. It indicated that the hydroxyl (-OH) and carbonyl (C=O) groups of GO facilitated rapid electron mobility. The non-functionalized Gr showed comparatively lesser degradation efficiency of degraded ~ 84 and 83.6%, respectively against MG and MB. On the other hand, Gr was found to be more effective to degrade the azoic MO dye (~ 74.5%) as compared to GO (~ 43.4 %). It might be due to the high recombination effect of functional groups present in GO with the azo-bonds (-N=N-), anions, dual phenyl rings and multiple bonds within MO, leading to poor degradation efficiency. While the absence of functional groups in Gr resulted in low recombination effect thereby showing comparatively high degradation efficiency. However, the photodegradation of 1:1:1 mixture of MG:MB:MO (dye cocktail) was studied in

presence of GO, separated in HPLC to estimate the degradation efficiency of each dye. In the real-time application the growth of *Lemna Minor* which failed up to 15<sup>th</sup> day in presence of dye mixture, found to proliferate rapidly in presence of GO treated dye mixture on the 20<sup>th</sup> day. Similar results were also observed in case of *Eichhornia crassipes*.

#### ACKNOWLEDGEMENT

The authors like to thank Department of Veterinary Pharmacology & Toxicology, West Bengal University of Animal & Fishery Sciences, Kolkata for the photodegradation studies involving UV-Vis Spectrophotometer and HPLC. The authors are highly obligated to Kris Biotech Research Pvt. Ltd., Kalyani for LC-MS/MS analysis of the dye fragments.

#### CONFLICT OF INTEREST

The authors declare no conflict of interest associated with this work.

#### REFERENCES

1. Mandal, P., Debbarma, J., Saha, M., "Critical Review on the Photodegradation Ability of Graphene and its derivatives against Malachite Green, Methylene Blue, and Methyl Orange", *Lett. Appl. NanoBioScience*, 12 (2023) 6.
2. Mandal, P., Nath, K. K., Saha, M., "Efficient Blue Luminescent Graphene Quantum Dots and their Photocatalytic Ability Under Visible Light", *Biointerface Res. Appl. Chem.*, 11 (2021) 8171-8178.
3. Ramesh, A. M., Gangadhar, A., Chikkamadaiah, M., Krishnegowda, J., Shivanna, S., "Synthesis of graphene nanosheets by emitted black carbon and its sustainable applications", *J. Environ. Chem. Eng.*, 8 (2020) 104071.
4. Karimi, H., Rajabi, H. R., Kavoshi, L., "Application of decorated magnetic nanophotocatalysts for efficient photodegradation of organic dye: A comparison study on photocatalytic activity of magnetic zinc sulfide and graphene quantum dots", *J. Photochem. Photobiol. A: Chem.*, 397 (2020) 112534.
5. Mandal, P., Debbarma, J., Saha, M., "A Review on the Emergence of Graphene in Photovoltaics Industry", *Biointerface Res. Appl. Chem.*, 11. (2021) 15009.
6. Mandal, P., Saha, M., "Synthesis of Graphene Nanosheets and Photocatalytic Application in Dye Degradation", *J. Sci. Ind. Res.*, 78 (2019) 863-867.
7. Raju, S., Ashok, D., Boddu, A. R., "Leucaena Leucocephala Mediated Green Synthesis of Silver Nanoparticles and Their Antibacterial, Dye Degradation and Antioxidant Properties", *Int. J. Nanosci. Nanotechnol.*, 18 (2022) 65-78.
8. Mirsadeghi, S., Zandavar, H., Rahimi, M., Tooski, H. F., Rajabi, H. R., Rahimi-Nasrabadi, M., Sohoul, E., Larijani, B., Pourmortazavi, S. M., "Photocatalytic reduction of imatinib mesylate and imipenem on electrochemical synthesized Al<sub>2</sub>W<sub>3</sub>O<sub>12</sub> nanoparticle: optimization, investigation of electrocatalytic and antimicrobial activity", *Colloids Surf. A Physicochem. Eng. Asp.*, 586 (2020) 124254.
9. Rajabi, H.R., Karimi, F., Kazemdehdashti, H., Kavoshi, L., "Fast sonochemically-assisted synthesis of pure and doped zinc sulfide quantum dots and their applicability in organic dye removal from aqueous media", *J. Photochem. Photobiol. B: Biol.*, 181 (2018) 98-105.
10. Heydari, S., Shirmohammadi Aliakbarkhani, Z., Hosseinpour Zaryabi, M., "Photocatalytic Degradation of SafraninDye from Aqueous Solution Using Nickel Nanoparticles Synthesized by PlantLeaves ", *Int. J. Nanosci. Nanotechnol.*, 16 (2020) 153-165.

11. Karimi, F., Rajabi, H. R., Kavoshi, L., "Rapid sonochemical water-based synthesis of functionalized zinc sulfide quantum dots: study of capping agent effect on photocatalytic activity", *Ultrason. Sonochem.*, 57 (2019) 139-146.
12. Sengupta, S., Pari, A., Biswas, L., Shit, P., Bhattacharyya, K., Chattopadhyay, A. P., "Adsorption of Arsenic on Graphene Oxide, Reduced Graphene Oxide, and their Fe<sub>3</sub>O<sub>4</sub> Doped Nanocomposites", *Biointerface Res. Appl. Chem.*, 12 (2022) 6196 - 6210.
13. Monsef Khoshhesab, Z., Ayazi, Z., Dargahi, M., "Synthesis of Magnetic Graphene Oxide Nanocomposite for Adsorption Removal of Reactive Red 1950 Modelling and : Optimizing via Central Composite Design", *Int. J. Nanosci. Nanotechnol.*, 16 (2020) 35-48.
14. Badry, R., Hegazy, M. A., Yahia, I. S., Elhaes, H., Zahran, H. Y., Ibrahim, M. A., "Effect of Zinc Oxide on the Optical Properties of Polyvinyl Alcohol/Graphene Oxide Nanocomposite", *Biointerface Res. Appl. Chem.*, 13 (2023) 39.
15. Uddin, M. J., Ampiaiw, R. E., Lee, W., "Adsorptive removal of dyes from wastewater using a metal-organic framework: A review", *Chemosphere*, 284 (2021) 131314.
16. Baena-Baldiris, D., Montes-Robledo, A., Baldiris-Avila, R., "Franconibacter sp., 1MS: A New Strain in Decolorization and Degradation of Azo Dyes Ponceau S Red and Methyl Orange", *ACS Omega*, 5 (2020) 28146-28157.
17. Sharma, J., Sharma, S., Soni, V., "Classification and impact of synthetic textile dyes on Aquatic Flora: A review", *Reg. Stud. Mar. Sci.*, 45 (2021) 101802.
18. Dubreil, E., Mompelat, S., Kromer, V., Guitton, Y., Danion, M., Morin, T., Hurtaud-Pessel, D., Verdon, E., "Dye residues in aquaculture products: targeted and metabolomics mass spectrometric approaches to track their abuse", *Food Chem.*, 294 (2019) 355-367.
19. Alwera, S., Talismanov, V. S., Alwera, V., Domyati, D., "Synthesis and Characterization of Sn-Doped CeO<sub>2</sub>-Fe<sub>2</sub>O<sub>3</sub> Nanocomposite and Application in Photocatalytic Degradation of Sudan I", *Biointerface Res. Appl. Chem.*, 13 (2023) 179.
20. Sahoo, J. K., Hota, A., Khuntia, A. K., Sahu, S., Sahoo, S. K., Sabar, A. K., Pani, S. K., Rath, J., "Removal of Dyes Using Various Organic Peel-based Materials: A Systematic Review", *Lett. Appl. NanoBioScience*, 11 (2022) 3714-3727.
21. Ma, J., Hou, L., Li, P., Zhang, S., Zheng, X., "Modified fruit pericarp as an effective biosorbent for removing azo dye from aqueous solution: study of adsorption properties and mechanisms", *Environ. Eng. Res.*, 27 (2022) 200634.
22. Mishra, S.P., Patra, A.R., Das, S., "Methylene blue and malachite green removal from aqueous solution using waste activated carbon", *Biointerface Res. Appl. Chem.*, 11 (2020) 7410-7421.
23. Vutskits, L., Briner, A., Klausner, P., Gascon, E., Dayer, A. G., Kiss, J. Z., Muller, D., Licker, M. J., Morel, D. R., "Adverse effects of methylene blue on the central nervous system", *J. Am. Soc. Anesthesiologists*, 108 (2008) 684-692.
24. Stamatii, A., Nebbia, C., De Angelis, I., Albo, A. G., Carletti, M., Rebecchi, C., Zampaglioni, F., Dacasto, M., "Effects of malachite green (MG) and its major metabolite, leucomalachite green (LMG), in two human cell lines", *Toxicol. in vitro*, 19 (2005) 853-858.
25. El-Naggar, N. E.-A., Hamouda, R. A., Saddiq, A. A., Alkinani, M. H., "Simultaneous bioremediation of cationic copper ions and anionic methyl orange azo dye by brown marine alga *Fucus vesiculosus*", *Sci. Rep.*, 11 (2021) 1-19.
26. Kumbhakar, D. V., Datta, A. K., Das, D., Ghosh, B., Pramanik, A., Gupta, S., "Assessment of cytotoxicity and cellular apoptosis induced by azo-dyes (methyl orange and malachite green) and heavy metals (cadmium and lead) using *Nigella sativa* L.(black cumin)", *Cytologia*, 83 (2018) 331-336.
27. Mandal, P., Saha, M., "Low-temperature synthesis of graphene derivatives: mechanism and characterization", *Chem. Pap.*, 73 (2019) 1997-2006.
28. Oppong, S. O.-B., Opoku, F., Govender, P. P., "Remarkable Enhancement of Eu-TiO<sub>2</sub>-GO Composite for Photodegradation of Indigo Carmine: A Design Method Based on Computational and Experimental Perspectives", *Catal. Lett.*, 151 (2021) 1111-1126.
29. Kolli, V.K., Mandal, P., "Experimental exploration of additive NGQD as a performance and emissions improver of the CI engine with biodiesel-diesel blends", *Int. J. Environ. Sci. Technol.*, 18 (2021)1-16.
30. Yeh, T.-F., Cihlár, J., Chang, C.-Y., Cheng, C., Teng, H., "Roles of graphene oxide in photocatalytic water splitting", *Mat. Today*, 16 (2013) 78-84.
31. Fu, T., Tang, X., Cai, Z., Zuo, Y., Tang, Y., Zhao, X., "Correlation research of phase angle variation and coating performance by means of Pearson's correlation coefficient", *Prog. Org. Coat.*, 139 (2020) 105459.
32. Roberts, G., Satterfield, C. "Effectiveness factor for porous catalysts. Langmuir-Hinshelwood kinetic expressions", *Ind. Eng. Chem. Res.*, 4 (1965) 288-293.

33. Chen, H., Liu, T., Meng, Y., Cheng, Y., Lu, J., Wang, H., "Novel graphene oxide/aminated lignin aerogels for enhanced adsorption of malachite green in wastewater", *Colloids Surf. A Physicochem. Eng. Asp.*, 603 (2020) 125281.
34. Gautam, D., Hooda, S., "Magnetic Graphene Oxide/Chitin Nanocomposites for Efficient Adsorption of Methylene Blue and Crystal Violet from Aqueous Solutions", *J. Chem. Eng. Data*, 65 (2020) 4052-4062.
35. El-Barbary, G., Ahmed, M.K., El-Desoky, M.M., Al-Enizi, A.M., Alothman, A.A., Alotaibi, A.M., Nafady, A., "Cellulose acetate nanofibers embedded with Ag nanoparticles/CdSe/graphene oxide composite for degradation of methylene blue", *Syn. Met.*, 278 (2021) 116824.
36. Qiao, W., Liu, H. "Enhanced decolorization of malachite green by a magnetic graphene oxide-CotA laccase composite", *Int. J. Biol. Macromol.*, 138 (2019) 1-12.
37. Ghattavi, S., Nezamzadeh-Ejhi, A., "GC-MASS detection of methyl orange degradation intermediates by AgBr/g-C<sub>3</sub>N<sub>4</sub>: Experimental design, bandgap study, and characterization of the catalyst", *Int. J. Hydrog. Energy*, 45 (2020) 24636-24656.
38. Ansorgová, D., Holčápek, M., Jandera, P., "Ion-pairing high-performance liquid chromatography-mass spectrometry of impurities and reduction products of sulphonated azodyes", *J. Sep. Sci.*, 26 (2003) 1017-1027.
39. Li, W., Li, D., Lin, Y., Wang, P., Chen, W., Fu, X., Shao, Y., "Evidence for the active species involved in the photodegradation process of methyl orange on TiO<sub>2</sub>", *J. Phys. Chem. C*, 116 (2012) 3552-3560.
40. Xu, Y.-H., Liang, D.-H., Liu, D.-Z., "Preparation and characterization of Cu<sub>2</sub>O-TiO<sub>2</sub>: efficient photocatalytic degradation of methylene blue", *Mater. Res. Bull.*, 43 (2008) 3474-3482.
41. Alam, U., Khan, A., Ali, D., Bahnemann, D., Muneer, M., "Comparative photocatalytic activity of sol-gel derived rare earth metal (La, Nd, Sm and Dy)-doped ZnO photocatalysts for degradation of dyes", *RSC Adv.*, 8 (2018) 17582-17594.
42. Chaudhary, R. P., Pawar, P. B., Vaibhav, K., Saxena, S., Shukla, S., "Quantification of adsorption of azo dye molecules on graphene oxide using optical spectroscopy", *JOM*, 69 (2017) 236-240.
43. Aboamra, N. M., Mohamed, A., Salama, A., Osman, T., Khattab, A., "An effective removal of organic dyes using surface functionalized cellulose acetate/graphene oxide composite nanofibers", *Cellulose*, 25 (2018) 4155-4166.
44. Gong, J., Gao, X., Li, M., Nie, Q., Pan, W., Liu, R., "Dye adsorption on electrochemical exfoliated graphene oxide nanosheets: pH influence, kinetics and equilibrium in aqueous solution", *Int. J. Environ. Sci. Technol.*, 14 (2017) 305-314.
45. Nas, M. S., Calimli, M. H., Burhan, H., Yilmaz, M., Mustafaov, S. D., Sen, F., "Synthesis, characterization, kinetics and adsorption properties of Pt-Co@ GO nano-adsorbent for methylene blue removal in the aquatic mediums using ultrasonic process systems", *J. Mol. Liq.*, 296 (2019) 112100.
46. Ju, Y., Yang, S., Ding, Y., Sun, C., Zhang, A., Wang, L., "Microwave-assisted rapid photocatalytic degradation of malachite green in TiO<sub>2</sub> suspensions: mechanism and pathways", *J. Phys. Chem. A*, 112 (2008) 11172-11177.
47. Ray, S. K., Dhakal, D., Lee, S. W., "Insight Into Malachite Green Degradation, Mechanism and Pathways by Morphology-Tuned  $\alpha$ -NiMoO<sub>4</sub> Photocatalyst", *Photochem. Photobiol.*, 94 (2018) 552-563.
48. Ju, Y., Yang, S., Ding, Y., Sun, C., Gu, C., He, Z., Qin, C., He, H., Xu, B., "Microwave-enhanced H<sub>2</sub>O<sub>2</sub>-based process for treating aqueous malachite green solutions: intermediates and degradation mechanism", *J. Hazard. Mater.*, 171 (2009) 123-132.
49. Pérez-Estrada, L., Agüera, A., Hernando, M., Malato, S., Fernández-Alba, A., "Photodegradation of malachite green under natural sunlight irradiation: kinetic and toxicity of the transformation products", *Chemosphere*, 70 (2008) 2068-2075.
50. Krishnan, S., Shriwastav, A., "Application of TiO<sub>2</sub> nanoparticles sensitized with natural chlorophyll pigments as catalyst for visible light photocatalytic degradation of methylene blue", *J. Environ. Chem. Eng.*, 9 (2021) 104699.
51. Zhao, Y., Zhang, Y., Liu, A., Wei, Z., Liu, S., "Construction of three-dimensional hemin-functionalized graphene hydrogel with high mechanical stability and adsorption capacity for enhancing photodegradation of methylene blue", *ACS Appl. Mater. Interfaces*, 9 (2017) 4006-4014.
52. Ghaffari, M., Tan, P. Y., Oruc, M. E., Tan, O. K., Tse, M. S., Shannon, M., "Effect of ball milling on the characteristics of nano structure SrFeO<sub>3</sub> powder for photocatalytic degradation of methylene blue under visible light irradiation and its reaction kinetics", *Catal. Today*, 161 (2011) 70-77.
53. He, Y., Grieser, F., Ashokkumar, M., "The mechanism of sonophotocatalytic degradation of methyl orange and its products in aqueous solutions", *Ultrason. Sonochem.*, 18 (2011) 974-980.
54. Bilal, M., Rasheed, T., Iqbal, H. M., Hu, H., Wang, W., Zhang, X., "Novel characteristics of horseradish peroxidase immobilized onto the polyvinyl alcohol-alginate beads and its methyl orange degradation potential", *Int. J. Biol. Macromol.*, 105 (2017) 328-335.

55. Kaur, J., Singhal, S., "Facile synthesis of ZnO and transition metal doped ZnO nanoparticles for the photocatalytic degradation of Methyl Orange", *Ceram. Int.*, 40 (2014) 7417-7424.
56. Mandal, P., Saha, M., "Photodegradation Behaviour of Nitrogen-Containing Graphene Derivatives Towards Pollutant Dyes and Real-Time Assessment on Aquatic Weed", *Biointerface Res. Appl. Chem.*, 12 (2022) 4357-4373.
57. Avinash, G. P., Karthick, R. N. S., Bavani Latha, M., Arvind B. R. S., "Polymer Extraction from Processed Lignocellulosic Biomass Water Hyacinth (*Eichhornia crassipes*) for the Potential Biological Activities", *Biointerface Res. Appl. Chem.*, 11 (2021) 9218-9226.
58. Mohamed, S., Mahrous, A., Elshahat, R., Kassem, M., "Accumulation of Iron, Zinc and Lead by *Azolla pinnata* and *Lemna minor* and activity in contaminated water", *Egypt. J. Chem.*, 64 (2021) 5017-5030.
59. Priya, E. S., Selvan, P. S., "Water hyacinth (*Eichhornia crassipes*)—An efficient and economic adsorbent for textile effluent treatment—A review", *Arabian J. Chem.*, 10 (2017) S3548-S3558.
60. Madikizela, L. M., "Removal of organic pollutants in water using water hyacinth (*Eichhornia crassipes*)", *J. Environ. Manage.*, 295 (2021) 113153.